NIH Public Access
Author Manuscript
Nature. Author manuscript; available in PMC 2013 June 20.

Published in final edited form as:
Nature. 2012 November 1; 491(7422): 66–71. doi:10.1038/nature11525.

Generation of functional thyroid from embryonic stem cells

Francesco Antonica[1], **Dominika Figini Kasprzyk**[1], **Robert Opitz**[1], **Michelina Iacovino**[2], **Xiao-Hui Liao**[3], **Alexandra Mihaela Dumitrescu**[3], **Samuel Refetoff**[3,4], **Kathelijne Peremans**[5], **Mario Manto**[6], **Michael Kyba**[2], and **Sabine Costagliola**[1]

[1]IRIBHM (Institute of Interdisciplinary Research in Molecular Human Biology), Université Libre de Bruxelles, 808 route de Lennik, 1070 Brussels, Belgium.

[2]Lillehei Heart Institute and Department of Pediatrics, University of Minnesota, Minneapolis, MN, USA.

[3]Department of Medicine, The University of Chicago, Chicago, IL, USA.

[4]Departments of Pediatrics and Genetics, The University of Chicago, Chicago, IL, USA.

[5]Department of Veterinary Medical Imaging and Small Animal Orthopaedics, Faculty of Veterinary Medicine, Ghent University, Belgium.

[6]FNRS, ERASME, Université Libre de Bruxelles, 808 Route de Lennik, 1070 Brussels, Belgium.

Abstract

The primary function of thyroid gland is to metabolize iodide by synthesizing thyroid hormones that are critical regulators of growth, development and metabolism in virtually all tissues. To date, research on thyroid morphogenesis was missing an efficient stem-cell model system which allows to recapitulate *in vitro* the molecular and morphogenic events regulating thyroid follicular cells differentiation and subsequent assembly into functional thyroid follicles. Here we report that a transient overexpression of the transcription factors NKX2.1 and PAX8 is sufficient to direct mouse embryonic stem-cells (mESC) differentiation into thyroid follicular cells which organized into three-dimensional follicular structures when treated with thyrotropin. Those in vitro derived follicles showed significant iodide organification activity. Importantly, when grafted *in vivo* into athyreoid mice, these follicles rescued thyroid hormone plasma levels and promoted subsequent symptomatic recovery. Thus, mESC can be induced to differentiate into thyroid follicular cells *in vitro* and generate functional thyroid tissue.

The mammal thyroid consists of two endocrine cell types, the thyroid follicular cells (TFC) that produce the thyroid hormones T3 and T4 and the C-cells that produce calcitonin[1]. In the adult thyroid gland, TFC are organized in follicular structures[2], where a monolayer of polarized TFC encloses a luminal compartment that is filled with a colloidal mass that contains thyroid hormone precursors bound to thyroglobulin[3]. A follicular organization of

Correspondence and requests for materials should be addressed to S.C. (scostag@ulb.ac.be).

Supplementary Information
11 Supplementary Figures and Legends

Author Contributions
F.A. and S.C. developed the project, designed the experiments and analysed the data. F.A. performed most of the *in vitro* experiments and *in vivo* studies. D.F.K. provided technical help for the *in vitro* differentiation and functional characterization of the cells. M.I and M.K. provided A2lox-Cre ESCs. X.H.L. analysed blood TSH levels. A.M.D. read carefully the manuscript and made experimental suggestions. S.R. provided suggestions and critical advice on the experimental procedures. K.P. performed whole-body scan. M.M. performed body temperature measurements. F.A., R.O. and S.C. wrote the manuscript. All authors read and approved the final manuscript.

The authors declare they have no competing financial interests.

NIH-PA Author Manuscript
NIH-PA Author Manuscript
NIH-PA Author Manuscript

NIH-PA Author Manuscript

NIH-PA Author Manuscript

NIH-PA Author Manuscript

TFC is considered the prerequisite for efficient thyroid hormone biosynthesis[4]. It has been demonstrated that NKX2.1[5] and PAX8[6] function are vital for TFC survival, differentiation[2] and function during thyroid organogenesis and in mature thyroid tissue[1]. During thyroid organogenesis, the onset of NKX2.1[7] and PAX8[8] co-expression in a small group of ventral foregut endodermal cells represents the first molecular marker of cell specification towards a TFC fate. Although NKX2.1[7] and PAX8[8] are individually expressed in a variety of tissues and cell types, their co-expression is restricted to cells committed to differentiate into TFC. Induced overexpression of defined transcription factors has been shown to have a directing effect on the differentiation of Embryonic Stem Cells (ESCs) into specific cell types[9–11]. Despite the success of this experimental approach for cell differentiation or reprogramming, protocols promoting coordinated self-assembly of differentiated cells into distinct morphological units with functional properties reminiscent of organs and tissues in vivo[12–14] are still very sparse. In this study, we explored whether overexpression of the two transcription factors NKX2.1 and PAX8 could promote differentiation of murine ESC (mESC) into TFC and subsequent self-formation of thyroid follicles.

In vitro thyroid cells differentiation

Because the factors and signaling pathways inducing concurrent expression of NKX2.1 and PAX8 have not yet been resolved[2], we generated recombinant mESC lines (Fig. 1a; Supplementary Fig. 1a,c,e) in which expression of these transcription factors can be temporally induced upon addition of doxycycline (Dox, 1 μg/ml) to the medium[15] (Supplementary Fig. 1b,d,f). These genetic manipulations did not affect the pluripotent state of the mESC (Supplementary Fig. 1g). In our experimental setup, Dox induction of NKX2.1 and PAX8 was initiated after a 4-day mESC culture in hanging drops to allow for differentiation into Embryoid Bodies (EBs) (Fig. 1b). We first used a recombinant mESC line in which Dox treatment induces NKX2.1+PAX8 overexpression (Supplementary Fig. 1a,b). After 3 days of Dox treatment (day 4 to day 7), co-expression of NKX2.1 and PAX8 was detectable by immunofluorescence in almost all Dox-treated cells on day 7 but never in cells incubated in the absence of Dox (Supplementary Fig. 2a). To determine whether the combined activity of NKX2.1 and PAX8 promotes TFC differentiation, we first examined the expression of various TFC markers by RT-qPCR. Strikingly, mRNA expression of functional markers including TSH receptor (*Tshr*), sodium/iodide symporter NIS (*Slc5a5*) and thyroglobulin (*Tg*) was strongly up-regulated within 3 days of Dox treatment, (Supplementary Fig. 2b). Notably, expression of *Foxe1*, another key transcription factor for thyroid development[16], was also up-regulated (Supplementary Fig. 2b) and $NKX2.1^{+}FOXE1^{+}$ cells were prominent throughout cell cultures (Supplementary Fig. 2c). Interestingly, our RT-qPCR analyses also demonstrated a robust increase of endogenous *Nkx2.1* and *Pax8* mRNA levels (Supplementary Fig. 2d) indicating an autoinduction of these transcription factors. Together, these data demonstrate that forced co-expression of NKX2.1 and PAX8 readily acts on cell fate driving the differentiation towards a TFC lineage. However, assembly of Dox-treated cells into three-dimensional aggregates reminiscent of follicle-like epithelial structures was rarely observed under these conditions. This was true for cell cultures employing a variety of distinct Dox treatment protocols, suggesting that additional factors might be required to promote follicular morphogenesis. We therefore revised the treatment protocol based on two critical observations. First, we limited the Dox treatment to a 3-day period from day 4 to day 7 (Fig. 1b) as this appeared to be sufficient to induce an autoinduction of endogenous *Nkx2.1* and *Pax8* mRNA expression. Second, we treated cells from day 7 onwards with recombinant human TSH (1 mU ml^{-1}) (Fig. 1b) as the robust up-regulation of *Tshr* mRNA suggested that cells had acquired a competence to respond to rhTSH. When using this sequential Dox-rhTSH treatment schedule, RT-qPCR analyses of day 22 cell cultures showed indeed a sustained elevation of endogenous *Nkx2.1* and *Pax8* mRNA expression (Fig.1c and Supplementary Fig. 3a, b).

NIH-PA Author Manuscript

NIH-PA Author Manuscript

NIH-PA Author Manuscript

Moreover, these cell cultures also showed a high expression of functional TFC markers such as *Tshr*, *Slc5a5*, *Tg* and *Tpo* (encoding for thyroid peroxidase) (Fig. 1c and Supplementary Fig. 3a, b). Immunofluorescence analyses at day 22 demonstrated that the sequential Dox-rhTSH treatment clearly promoted the differentiation of $NKX2.1^+$ cells co-expressing PAX8 (Fig. 1h; Supplementary Fig. 3g, k), FOXE1 (Fig. 1i; Supplementary Fig. 3h, l), NIS (Fig. 1j; Supplementary Fig. 3i, m) and TG (Fig. 1k; Supplementary Fig. 3j, n). No such co-expression was seen in absence of Dox-induced transgene expression (Fig. 1d–g; Supplementary Fig. 3c–f). The efficiency of TFC differentiation quantified as percentage of $NKX2.1^+PAX8^+$ cells reached 60.5 ± 8.1 % in the sequential Dox-rhTSH treatment protocol (mean ± s.e.m, $n = 3$; see methods). Most importantly, and in contrast to a 3-day Dox treatment without subsequent TSH treatment, the sequential Dox-rhTSH treatment greatly stimulated the assembly of TFC-like cells into distinct three-dimensional structures reminiscent of thyroid follicles (Supplementary Fig. 3, k–n; compare to Supplementary Fig. 3, g–j).

In vitro formation of functional follicles

A follicular organization of TFC is considered the prerequisite for thyroid hormone biosynthesis, which occurs under physiological conditions extra-cellularly at the TFC-colloid interface. Iodide organification requires a complex biosynthetic machinery including NIS-mediated iodide uptake[17] at the basal pole[18], TG synthesis and targeting to the apical pole, H_2O_2 generation at the TFC-colloid interface by dual oxidase and TPO-mediated iodination of TG[4] (Fig. 2a). Immunofluorescence analyses of the follicular aggregates demonstrated polarization characteristics consistent with thyroid follicles in intact animals (Fig. 2b). The $NKX2.1^+$ cells surrounding a luminal space displayed basolateral localization of NIS (Fig. 2c) and E-cadherin (Fig. 2d) as well as apical localization of zona occludens 1 (ZO-1) (Fig. 2e). TG immunofluorescence, on the other hand, was observed both intracellularly and in the luminal compartment (Fig. 2f). It should be noted that neither endothelial cells nor C-cells were observed after 22 days of cell culture, as judged by the absence of detectable PECAM-1 and calcitonin staining respectively. Together, these data demonstrate the efficiency of the sequential Dox-rhTSH treatment to generate cells with a molecular signature highly similar to TFC and to promote the assembly of these TFC-like cells into three-dimensional follicular structures strongly resembling thyroid follicles. We next asked whether Dox induction of either NKX2.1 or PAX8 alone is sufficient to promote TFC differentiation and follicle morphogenesis. Dox induction of NKX2.1 alone for 3 days was sufficient to up-regulate expression of various TFC markers as assessed by RT-qPCR (Supplementary Fig. 4a, b) and by immunostaining for PAX8 (Supplementary Fig. 4c) and FOXE1 (Supplementary Fig. 4d). However, with the exception of *Pax8* mRNA expression, the effects of NKX2.1 overexpression were weaker relative to Dox induction of NKX2.1+PAX8 (Supplementary Fig. 2b) and no up-regulation was evident for endogenous *Nkx2.1a* mRNA (Supplementary Fig. 4a). When using the sequential Dox-rhTSH protocol, NKX2.1 induction was clearly sufficient to promote differentiation towards a TFC-like cell fate (Fig. 1c and Fig. 1l–o) but failed to efficiently promote formation of follicle-like cell aggregates (compare Fig. 1k and Fig. 1o). Given the vital role of TSH treatment for folliculogenesis as observed in the NKX2.1+PAX8 overexpression model, the comparatively low level of *Tshr* up-regulation induced by overexpression of NKX2.1 might represent one plausible factor explaining the lack of follicle morphogenesis in the NKX2.1 overexpression model (see Fig. 1c; Supplementary Fig. 4a,b). In striking contrast to NKX2.1 overexpression, Dox induction of PAX8 had only marginal effects on TFC marker expression, both at the level of mRNA (Supplementary Fig. 5a,b) and protein expression (Supplementary Fig. 5c,d). Treatment with rhTSH after Dox induction of PAX8 did not promote TFC differentiation as judged from day 22 analyses of TCF marker gene expression (Fig. 1c) and immunofluorescence staining (Fig. 1p–s). Together, these data indicate that

NIH-PA Author Manuscript

NIH-PA Author Manuscript

NIH-PA Author Manuscript

transient NKX2.1 overexpression is sufficient to drive cell differentiation towards the TFC lineage. PAX8, on the other hand, did not promote TFC differentiation when overexpressed alone but strongly enhanced TFC differentiation when overexpressed together with NKX2.1. Most importantly, overexpression of both NKX2.1 and PAX8 was a critical requirement for the rhTSH-dependent self-assembly of TFC into into follicle-like structures. The high similarity between in vitro-generated follicle-like structures and true thyroid follicles, both at the molecular and morphological level, prompted us to examine whether these follicular structures were functional for the two hallmarks of thyroid tissue: iodide trapping and thyroid hormone synthesis. We therefore assessed day 22 cell cultures derived by the sequential Dox-rhTSH protocol for their capacity to organify iodide. First evidence for active iodide organification was obtained by immunofluorescence detection of iodinated TG (TG-I) within the luminal compartment of follicular aggregates (Fig. 2g) using an antibody that selectively recognizes iodinated TG epitopes[19]. Positive TG-I staining was limited to cell cultures obtained after Dox induction of NKX2.1+PAX8 and subsequent rhTSH treatment. We next used a “classical” iodide organification assay that measures the relative incorporation of radioiodine into TCA-precipitable proteins after 2 hours of incubation in a [^{125}I]-supplemented medium. Measurements of radioiodine incorporation corroborated the TG-I staining results as a strong and significant increase of iodide organification was exclusively seen in cell cultures upon Dox induction of NKX2.1+PAX8 and subsequent rhTSH treatment (Fig. 2h–j and Supplementary Fig. 6). The capacity of such cell cultures for significant iodide organification is in line with their TFC-like molecular signature and their three-dimensional follicular organization. In turn, the lack of similar functional properties of cell cultures derived after induction of either NKX2.1 (Fig. 2i) or PAX8 alone (Fig. 2j) would be consistent with a failure of TFC differentiation (Dox induction of PAX8 alone) or the reduced competence to form follicular aggregates upon rhTSH treatment (Dox induction of NKX2.1 alone). Together, our data demonstrate that the differentiation protocol relying on overexpression of NKX2.1+PAX8 allows deriving *in vitro* follicular organoid structures that recapitulate molecular, morphological and functional properties of *bona fide* thyroid follicles. In addition, this protocol highlights the vital role of TSH to complete the process of follicular maturation.

In vivo functionality of derived follicles

To assess the potential *in vivo* functionality of the mESC-derived thyroid follicles, we grafted follicular organoids under the kidney capsules of female mice previously made hypothyroid by i.p. [^{131}I] injection (Fig. 3a). Histological evaluation of the kidney region one month after transplantation demonstrated successful integration of grafted organoids in the host niche (Fig. 3b, c). At the grafting site, (Fig. 3b), numerous follicles containing a monolayered epithelium were present at the cortical area of the host organ (Fig. 3c and Supplementary Fig. 7a). *In situ* chromosome Y painting on paraffin sections of the grafting region provided clear evidence that the follicular structures originated from male mESC-derived organoids, on a background of female kidney tissue of the hosts (Supplementary Fig. 8a,b). Immunostaining demonstrated that the follicular epithelium was made up of cells positive for NKX2.1 (Fig. 3d), PAX8 (Fig. 3e) and FOXE1 (Fig. 3f), a molecular signature highly similar to the thyrocytes of orthotopic thyroid tissue. Further immunohistochemical analyses corroborated the development of functional thyroid follicles at the grafting sites including cytosolic TG expression and TG deposition in the luminal compartment (Fig. 3g), polarized NIS (Fig. 3h) and E-cadherin (Supplementary Fig. 7b) expression at the basolateral membrane as well as detection of the thyroid hormone T4 in the colloid (Fig. 3i and Supplementary Fig. 7a). Importantly, immunostaining for the pan-endothelial marker PECAM-1 showed that thyroid follicles were surrounded by a dense network of small blood vessels demonstrating the formation of classical angio-follicular units (Supplementary Fig. 7c,d). Lastly, we could not detect any calcitonin staining in the grafted tissue, while

NIH-PA Author Manuscript

NIH-PA Author Manuscript

NIH-PA Author Manuscript

calcitonin staining was clearly detectable in the orthotopic thyroid tissue of adult mice (data not shown). Thus, consistent with the proposed origin and migration path of C-cells[20], the ectopic thyroid tissue graft are free of C-cells, implicating that our differentiation protocol does not promote C-cell development.

Functional rescue in hypothyroid mice

We next evaluated the ability of the mESC-derived tissue grafts to restore thyroid homeostasis in mice with radioiodine-ablated thyroid tissue. Plasma T4 levels measured in female mice at one month after [^{131}I] injection revealed a severe hypothyroid status at the time when mESC-derived organoids were transplanted (Fig. 4a and Supplementary Fig. 9a). Four weeks after grafting (8 weeks after [^{131}I] injection), mice grafted with cells that were differentiated upon overexpression of NKX2.1+PAX8 and subsequent rhTSH treatment showed a substantial elevation of plasma T4 levels (Fig. 4b and Supplementary Fig. 9b), with a complete rescue of thyroid homeostasis being evident in 8 out of 9 animals. Notably, mice transplanted with cells that were differentiated without Dox and rhTSH treatment remained hypothyroid (Fig. 4b) as was the case for mice that received no grafts at all (Supplementary Fig. 9b). To demonstrate that the grafted thyroid tissue is responsible for the restoration of plasma T4 levels, we performed whole-body scintigraphy of mice after intramuscular injection of ^{99mTC}-pertechnetate a gamma emitter transported by the sodium-iodide symporter (Fig. 4c,d). As shown in Fig. 4c, strong ^{99mTC}-pertechnetate uptake was observed in control mice in the neck region (where thyroid and salivary glands reside), the stomach and the bladder. In athyreoid mice grafted with mESC-derived thyroid follicles, ^{99mTC}-pertechnetate uptake was dramatically decreased in the neck region, due to the absence of the thyroid gland (Fig. 4d). The remaining weak signal in the neck region is due to NIS activity in the salivary gland. Importantly, a very strong signal was detectable at the grafting site close to the kidney. These data provide strong evidence that the grafted tissue is responsible for restoration of plasma T4 levels. Along with the restoration of normal T4 plasma levels, mice grafted with mESC-derived thyroid follicles also show a progressive decrease of plasma TSH levels (Fig. 4e and Supplementary Fig. 9c). Moreover, acute TSH administration[21] to athyroid grafted mice was effective in producing an increase in circulating levels of T4, suggesting TSH responsiveness of the grafted tissue (Supplementary Fig. 10). To examine whether our grafting approach also resulted in a symptomatic recovery, we analysed body temperature in mice from the different treatment groups. Decreased body temperature was found to be a robust and sensitive response to lowered plasma thyroid hormone concentrations. Importantly, mice grafted with mESC-derived thyroid follicles showed a full normalization of body temperature at 4 weeks after transplantation, providing a compelling example for symptomatic recovery along with the normalization of plasma hormone concentrations (Fig. 4f and Supplementary Fig. 11). These *in vivo* data clearly demonstrate that mESC-derived thyroid follicles have potent functional capacity to compensate for the lack of orthotopic thyroid tissue allowing full rescue of experimentally induced hypothyroidism (Fig. 4g).

Conclusion and perspectives

In the present study, we have developed a protocol that allows for generation of functional thyroid follicles from mESC based on transient overexpression of two transcription factors followed by rhTSH treatment. Recently, elegant studies demonstrated self-formation of two ectoderm-derived complex organs, adenohypophysis[13] and optic cup[12], using three-dimensional mESC culture systems, as well as the capacity of colon stem cells to recapitulate *in vitro* the self-organization of an endoderm-derived tissue, the crypt-villus structures[22,23]. Although a few previous studies reported on the detection of thyrocyte-like cells in ESC cultures[24–27], the present study is the first to demonstrate self-formation of

NIH-PA Author Manuscript

NIH-PA Author Manuscript

NIH-PA Author Manuscript

thyroid follicles from mESC-derived TFC and their capacity for iodide organification *in vitro*. Importantly, when transplanted into mice, the mESC-derived cells generated functional thyroid tissue able to rescue thyroid hormone deficits in athyreoid animals. Particularly the latter finding of our study opens a new avenue for application of stem cell technologies in the treatment of hypothyroidism, an area that so far received relatively little attention in regenerative medicine. In this context, one should bear in mind that congenital hypothyroidism, resulting from either dysfunctional (15%) or dysplastic (85%) thyroid tissue, is the most common congenital endocrine disease in humans, affecting one of 2000 newborns[28].

Methods

ESC culture for maintenance and differentiation

A2lox.Cre mouse ESCs[15] were routinely propagated on γ-ray irradiated Murine Embryonic Fibroblasts in DMEM (Invitrogen) supplemented with 15% ES-certified Fetal Bovine Serum (Invitrogen), 0.1 mM non-essential amino acids (Invitrogen), 1 mM sodium pyruvate (Invitrogen), 0.1 mM 2-mercaptoethanol (Sigma), 50 U ml^{-1} penicillin / 50 μg ml^{-1} streptomycin (Invitrogen) and 1,000 U ml^{-1} LIF (ESGRO). EBs were differentiated as described previously[29]. Briefly, EBs, generated by culturing ESCs in hanging drops (1,000 cells per drop) for up to 4 days, were collected and embedded in GFR-Matrigel (BD Biosciences); 50 μl Matrigel drops (containing roughly 6 EBs per drop) were replated on 15 mm Ø glass coverslips into 12-well plates. EBs were differentiated and cultured using a differentiation medium previously described[29] but supplemented with 1 μg ml^{-1} doxycycline (Sigma) and 1 mU ml^{-1} rhTSH (Genzyme) when indicated.

Cell preparation for *in vivo* transplantation

Cells at day 22 of differentiation (grown in 12-well plates) were washed twice with Hanks's Balanced Salt Solution (HBSS containing Calcium and Magnesium, Invitrogen) and incubated with a digestion medium (1 ml per well) containing 10 U ml^{-1} Dispase II (Roche) and 125 U ml^{-1} Collagenase type IA (Sigma) in HBSS for 30 minutes at 37°C. Cells were gently dissociated, resuspended manually with a P1000 Gilson and collected in a 15 ml Falcon tube (12 wells per tube that represent roughly 72 EBs). Cells were rinsed twice with differentiation medium following centrifugation at 200 g for 3 minutes. Low speed centrifugation allowed the separation of aggregates (pellet mainly composed by thyroid follicles) and single cells (supernatant). Finally, each pellet was resuspended in 65 μl of differentiation medium and a volume of 8 μl was used for transplantation.

Generation of tetracycline-inducible ESC lines

The tetracycline-inducible *Nkx2.1* ESC line, *Pax8* ESC line and *Nkx2.1-Pax8* ESC line were generated according to previously described[10]. Briefly, the coding sequences of either *Nkx2.1* and *Pax8* separated by an IRES sequence (for A2lox *Nkx2.1-Pax8* ESC line) or only *Nkx2.1* (for A2lox *Nkx2.1* ESC line) or only *Pax8* (for A2lox *Pax8* ESC line) were cloned into p2Lox targeting vector in order to create the following vectors: p2lox-*Nkx2.1-Pax8,* p2lox-*Nkx2.1* and p2lox-*Pax8.* 5,000,000 mESCs were electroporated with the different p2Lox vectors allowing the unidirectional recombination of the transgene in the HPRT locus. Positive clones were isolated using 300 μg ml^{-1} neomycin (Invitrogen) selection. Clones were screened by immunofluorescence against NKX2.1 and PAX8 after 24 hours in the absence or presence of 1 μg ml^{-1} doxycycline to verify transgene expression.

NIH-PA Author Manuscript

NIH-PA Author Manuscript

NIH-PA Author Manuscript

RNA extraction and qRT-PCR

For total RNA preparation, cells were lysed in RNeasy Lysis buffer (Qiagen) + 1% 2-mercaptoethanol, and RNA was isolated using RNeasy RNA preparation microkit (Qiagen) according to manufacturer's instructions. Reverse transcription was done using Superscript II kit (Invitrogen). Quantitative PCR (qPCR) was performed in duplicate using Power SybrGreen mix and a 7500 Real-Time PCR System (Applied Biosystem). Results are presented as linearized values normalized to the housekeeping gene *TBP* and the indicated reference value ($2^{-\Delta\Delta Ct}$). Gene expression profile was confirmed in 2 different clones. Primers used were as follows: *TBP*, forward 5'-TGTACCGCAGCTTCAAAATATTGTAT-3', reverse 5'-AAATCAACGCAGTTGTCCGTG-3'; *Nkx2.1* (endogenous isoform), forward 5'-GGCGCCATGTCTTGTTCT-3', reverse 5'-GGGCTCAAGCGCATCTCA-3'; *Pax8* (endogenous isoform), forward 5'-CAGCCTGCTGAGTTCTCCAT-3', reverse 5'-CTGTCTCAGGCCAAGTCCTC-3'; *Foxe1*, forward 5'-GGCGGCATCTACAAGTTCAT-3', reverse 5'-GGATCTTGAGGAAGCAGTCG-3'; *Tshr*, forward 5'-GTCTGCCCAATATTTCCAGGATCTA-3', reverse 5'-GCTCTGTCAAGGCATCAGGGT-3'; *Slc5a5*, forward 5'-AGCTGCCAACACTTCCAGAG-3', reverse 5'-GATGAGAGCACCACAAAGCA-3'; *Tg*, forward 5'-GTCCAATGCCAAAATGATGGTC-3', reverse 5'-GAGAGCATCGGTGCTGTTAAT-3'; *Tpo*, forward 5'-ACAGTCACAGTTCTCCACGGATG-3', reverse 5'-ATCTCTATTGTTGCACGCCCC-3'.

Immunofluorescence and Immunohistochemistry

For immunofluorescence experiments, cells were fixed in 4% paraformaldehyde (Sigma) for 30 minutes and washed thrice in PBS. Cells were blocked in a solution of PBS containing 3% Bovine Serum Albumin (BSA, Sigma), 5% Horse Serum (HS, Invitrogen) and 0.3% Triton X-100 (Sigma) for 30 minutes at room temperature. The primary and secondary antibodies were diluted in a solution of PBS containing 3% BSA, 1% HS and 0.1% Triton X-100. Primary antibodies were incubated overnight at 4°C followed by incubation with secondary antibodies for 2 hours at RT. Nuclei were stained with Hoechst 33342 (Invitrogen). Coverslips were mounted with Glycergel (Dako). For histological examination, grafted animals, previously anaesthetized, were perfused with 4% paraformaldehyde and the explanted kidneys were fixed overnight in 4% paraformaldehyde. Tissues were processed for paraffin or Tissue-Tek O.C.T. Compound (Sakura) inclusion. Immunohistochemistry on paraffin-embedded tissue sections was performed as described previously[31]. OCT-embedded tissue sections were incubated in blocking buffer containing 5% HS, 1% BSA and 0.2% Triton X 100 in PBS for 1 hour at room temperature. Only for PECAM-1 immunostaining, a prior antigen retrieval was performed by incubating tissue sections in 0.1% Trypsin solution 30 minutes at 37°C. Primary antibodies were diluted in blocking solution and incubated overnight at 4°C (at room temperature for the anti-PECAM-1). Sections were rinsed three times in PBS and incubated with secondary antibodies diluted in blocking solution at 1:400 for 1 hour at room temperature. Nuclei were stained with Hoechst 33342 (Invitrogen) and slides were mounted with Glycergel (Dako).

Antibodies

Primary antibodies used were the following: mouse anti-NKX2.1 (clone 8G7G3/1 Invitrogen, 1:3,000), rabbit anti-NKX2.1 (PA 0100 Biopat, 1:3,000), rabbit anti-PAX8 (PA 0300 Biopat, 1:3,000), rabbit anti-FOXE1 (PA 0200 Biopat, 1:600), rabbit anti-Thyroglobulin (A0251 Dako, 1:3,000), rabbit anti-NIS (a gift from N. Carrasco 1:1,000), mouse anti-E-cadherin (610181 BD, 1:3,000; 1:200 for IHC on cryosections), mouse anti-ZO-1 (339100 Invitrogen, 1:750), rabbit anti-T4 (MP Biochemicals, 1:3,000), mouse anti-TG-I (a gift from C. Ris-Stalpers, 1:2,000), rat anti-PECAM-1 (557355 BD, 1:100), rabbit

NIH-PA Author Manuscript

NIH-PA Author Manuscript

NIH-PA Author Manuscript

anti-Calcitonin (A0576 Dako, 1:8000). Secondary antibodies were donkey anti-mouse, anti-rabbit and anti-rat IgG conjugated with DyLight-488, Cy3 and DyLight-647 (Jackson Immunoresearch), goat anti-chicken IgG conjugated with Alexa-488 (Invitrogen), donkey biotinylated anti-rabbit IgG (Jackson Immunoresearch).

FISH analysis

FISH analysis on paraffin-embedded tissue sections was modified from a previous description[32]. Briefly, sections, previously deparaffinised in toluene (three times, 5 minutes/each) and rehydrated through graded alcohols to water, were incubated in 1 M sodium thiocyanate (Sigma) for 10 minutes at 80°C, washed in PBS and then digested in 0.4% pepsin (Sigma, P7012) in 0.1 M HCl for 10 minutes at 37°C. Digestion was quenched in 0.2% glycine (Sigma) in 2X PBS, and then sections were rinsed twice in 1X PBS, post-fixed in 4% paraformaldehyde, washed thrice in 1X PBS and finally dehydrated through graded alcohols and air dried. The probe mixture was prepared according to manufacturer's instructions. Briefly, 3 μl of mouse IDetect Biotin-labelled chromosome Y paint probe (Stat-FISH, Cambio; IDMB1055) were diluted in 7 μl of supplied Hybridization buffer. The probe mixture was added to the sections, covered with glass coverslip (22×22 mm), sealed with rubber cement, and probes/sections were denaturated for 10 minutes at 60°C and then incubated overnight at 37°C in a humid chamber. The next day, detection of Y-chromosome was performed using "Biotin labelled chromosome detection protocol detect with Texas Red" (Star-FISH, Cambio; 1082-KT-50) according to manufacturer's instructions.

Iodide organification assay

Cells at day 22 of differentiation were washed with HBSS and incubated with 1 ml of an organification medium containing 1,000,000 cpm ml^{-1} [^{125}I] (PerkinElmer) and 100 nM sodium iodide (Sigma) in HBSS for 2 hours at 37°C. After addition of 1 ml 4 mM methimazole (MMI, Sigma), a TPO inhibitor, cells were washed with ice cold HBSS and detached by a solution containing 0.1% Trypsin (Invitrogen) and 1 mM EDTA (Invitrogen) in PBS for 15 minutes. Cells were collected in polyester tubes and radioactivity was measured by γ-counter, indicating the cell Iodide uptake. Subsequently proteins were precipitated twice by addition of 1 mg γ-Globulins (Sigma) and 2 ml 20% TCA followed by centrifugation at 2,000 rpm for 10 minutes and the radioactivity of protein-bound [^{125}I] (PBI) was measured by γ–counter. Iodide organification was calculated as Iodide uptake:PBI ratio and the values were expressed as %. Background protein-bound radioactivity was measured in cells incubated with organification medium supplemented with 2 mM MMI. Results were confirmed in 3 different clones for each ESC line.

Generation of induced-hypothyroidism mouse model and transplantation of ESC-derived thyroid follicles

All animal experiments and care were in compliance with institutional guidelines and local ethical committees. 129P2/OlaHsd mice (5-week-old females) were provided from Harlan Laboratory. Hypothyroidism mouse model was generated as described previously[30]. Briefly, experimental hypothyroidism was induced by administering 150 μCi of [^{131}I] by intraperitoneal injection to mice, which had been placed on a low-iodine diet (Custom iodine deficient food, SAFE) for 8 days. 4 weeks after the administration of [^{131}I], plasma levels of T4 were analysed to confirm the hypothyroid status. One week later (5th week), the hypothyroid mice were weighed and anaesthetized with 3 ml kg^{-1} of an anaesthetic solution composed of 20 mg ml^{-1} of ketamine (Ketalar® - Pfizer) and 2 mg ml^{-1} xylazine (Rompun® - Bayer) and then injected with a volume of 8 μl of Dox/rhTSH-treated or untreated day-22 cells into the unilateral kidney under the capsule using a 30G needle syringe (Hamilton Bonaduz AG) (the kidney was exposed by skin/muscle/peritoneum incision via the dorso-lateral approach). 4 weeks later (9th week), the grafted mice were

NIH-PA Author Manuscript

NIH-PA Author Manuscript

NIH-PA Author Manuscript

subjected to body temperature measurement, blood sampling for plasma T4 and TSH measurements, whole-body imaging and sacrifice for histological examination of the kidneys.

Body temperature measurement

Rectal temperature was measured in conscious mice using a highly sensitive dedicated sensor (Iso-Temp-2) connected to an Apollo-1000 unit (World Precision Instruments, UK). Animals were restrained and kept motionless to obtain a stable rectal temperature.

Plasma T4 and TSH level measurements

Total T4 level was assayed by a [^{125}I] radioimmunoassay (Coat-A-Count Canine T4, Siemens) according to manufacturer's instructions. TSH was measured in 50 μl of serum as described previously[33]. Labelled TSH was provided from Institute of Isotopes Co., Ltd, Konkoly-Thege M u.29–33, Hungary.

TSH stimulation test

TSH stimulation test was modified from a previous description[21]. Briefly, A single injection of 10 mU of bTSH (Sigma) was given ip to animals pre- treated for 4 days with 3 μg T3 (Sigma) per day. Blood sampling was performed before and 3 h after bTSH injection for the measurement of T4.

Whole-body planar imaging

In this study pertechnetate was used as it is a good indicator to demonstrate the presence of Na-I symporter. Approximately 30 minutes after im injection of 37 MBq (1 mCi) ^{99m}Tc-Pertechnetate in the thigh region, the scans were performed on a dual head gamma camera (Toshiba, GCA 7200 A) equipped with a low energy high resolution (LEHR) collimator. For this procedure mice were anesthetized with isoflurane and kept (Isoflo®, Abbott Laboratories, Queenborough, United Kingdom) (2 % end tidal concentration) with oxygen using a rebreathing system and a mask. One static image (acquisition time 10 minutes, matrix 128 × 128, zoom 3) was made in ventral recumbency.

Statistical Analysis

Statistical significance was tested as follows: two-group comparison by unpaired *t*-test and multiple-group comparison by the one-way ANOVA test with a post-hoc Tukey's Comparison Test. For quantification of NKX2.1 and PAX8 double positive cell numbers, at least 2,000 cells were counted in ten different fields from three biologically independent experiments.

Imaging

Fluorescence imaging was performed on a Zeiss LSM510 META confocal microscope, a Zeiss Axio Observer Z1 microscope with AxioCamMR3 camera and a Leica DMI6000 with DFC365FX camera. Images were processed with ImageJ. Bright-field imaging was performed on a Zeiss Axioplan2 microscope with the AxioCamHR camera. Images were processed with Axiovision release 4.8 software. Photoshop CS5 (Adobe) was used to adjust brightness, contrast and picture size.

Supplementary Material

Refer to Web version on PubMed Central for supplementary material.

NIH-PA Author Manuscript

NIH-PA Author Manuscript

NIH-PA Author Manuscript

Acknowledgments

We thank G. Vassart, C. Blanpain and P. Vanderhaeghen for fruitful discussions and comments on manuscript. We thank Véronique Janssens for technical help. X.H.L., A.M.D. and S.R. are supported in part by grants DK15070 and DK91016 from the National Institutes of Health, USA. This work was supported by the Belgian Fonds de la Recherche Scientifique Medicale (RSM[2]3_4_557_08 and [3]3_4598_12), by Action de Recherche Concertée de la Communauté Française de Belgique (ARC N°AUWB-08/13-ULB10), by Fonds d' Encouragement à la Recherche (ULB) and grants from the Belgian National Fund for Scientific Research (FNRS). F.A. and D.F.K. are FNRS/FRIA research fellows. R.O. is FNRS Postdoctoral Researcher and S.C. is FNRS Senior Research Associate.

References

1. De Felice M. Thyroid Development and Its Disorders: Genetics and Molecular Mechanisms. Endocrine Reviews. 2004; 25:722–746. [PubMed: 15466939]
2. De Felice M, Di Lauro R. Minireview: Intrinsic and Extrinsic Factors in Thyroid Gland Development: An Update. Endocrinology. 2011; 152:2948–2956. [PubMed: 21693675]
3. Mauchamp J, Mirrione A, Alquier C, Andre F. Follicle-like structure and polarized monolayer: role of the extracellular matrix on thyroid cell organization in primary culture. Biol Cell. 1998; 90:369–380. [PubMed: 9835011]
4. Nunez J, Pommier J. Formation of thyroid hormones. Vitam Horm. 1982; 39:175–229. [PubMed: 6755886]
5. Kimura S, et al. The T/ebp null mouse: thyroid-specific enhancer-binding protein is essential for the organogenesis of the thyroid, lung, ventral forebrain, and pituitary. Genes Dev. 1996; 10:60–69. [PubMed: 8557195]
6. Mansouri A, Chowdhury K, Gruss P. Follicular cells of the thyroid gland require Pax8 gene function. Nat Genet. 1998; 19:87–90. [PubMed: 9590297]
7. Lazzaro D, Price M, de Felice M, Di Lauro R. The transcription factor TTF-1 is expressed at the onset of thyroid and lung morphogenesis and in restricted regions of the foetal brain. Development. 1991; 113:1093–1104. [PubMed: 1811929]
8. Plachov D, et al. Pax8, a murine paired box gene expressed in the developing excretory system and thyroid gland. Development. 1990; 110:643–651. [PubMed: 1723950]
9. Kyba M, Perlingeiro RC, Daley GQ. HoxB4 confers definitive lymphoid-myeloid engraftment potential on embryonic stem cell and yolk sac hematopoietic progenitors. Cell. 2002; 109:29–37. [PubMed: 11955444]
10. Ahfeldt T, et al. Programming human pluripotent stem cells into white and brown adipocytes. Nat Cell Biol. 2012; 14:209–219. [PubMed: 22246346]
11. Kamiya D, et al. Intrinsic transition of embryonic stem-cell differentiation into neural progenitors. Nature. 2011; 470:503–509. [PubMed: 21326203]
12. Eiraku M, et al. Self-organizing optic-cup morphogenesis in three-dimensional culture. Nature. 2011; 472:51–56. [PubMed: 21475194]
13. Suga H, et al. Self-formation of functional adenohypophysis in three-dimensional culture. Nature. 2011; 480:57–62. [PubMed: 22080957]
14. Eiraku M, Sasai Y. Mouse embryonic stem cell culture for generation of three-dimensional retinal and cortical tissues. Nat Protoc. 2012; 7:69–79. [PubMed: 22179593]
15. Iacovino M, et al. Inducible cassette exchange: a rapid and efficient system enabling conditional gene expression in embryonic stem and primary cells. Stem Cells. 2011; 29:1580–1588. [PubMed: 22039605]
16. De Felice M, et al. A mouse model for hereditary thyroid dysgenesis and cleft palate. Nat Genet. 1998; 19:395–398. [PubMed: 9697704]
17. Dai G, Levy O, Carrasco N. Cloning and characterization of the thyroid iodide transporter. Nature. 1996; 379:458–460. [PubMed: 8559252]
18. Carrasco N. Iodide transport in the thyroid gland. Biochim Biophys Acta. 1993; 1154:65–82. [PubMed: 8507647]
19. Hartog MTD, Boer MD, Veenboer GJM, Vijlder JJMD. Generation and Characterization of Monoclonal Antibodies Directed against Noniodinated and Iodinated Thyroglobulin, among which

NIH-PA Author Manuscript

NIH-PA Author Manuscript

NIH-PA Author Manuscript

Are Antibodies against Hormonogenic Sites. Endocrinology. 1990; 127:3160–3165. [PubMed: 2249644]

20. Fontaine J. Multistep migration of calcitonin cell precursors during ontogeny of the mouse pharynx. Gen Comp Endocrinol. 1979; 37:81–92. [PubMed: 437500]
21. Moeller LC, et al. Hypothyroidism in thyroid transcription factor 1 haploinsufficiency is caused by reduced expression of the thyroid-stimulating hormone receptor. Mol Endocrinol. 2003; 17:2295–2302. [PubMed: 12907760]
22. Sato T, et al. Single Lgr5 stem cells build crypt-villus structures in vitro without a mesenchymal niche. Nature. 2009; 459:262–265. [PubMed: 19329995]
23. Yui S, et al. Functional engraftment of colon epithelium expanded in vitro from a single adult Lgr5(+) stem cell. Nat Med. 2012; 18:618–623. [PubMed: 22406745]
24. Lin RY, Kubo A, Keller GM, Davies TF. Committing embryonic stem cells to differentiate into thyrocyte-like cells in vitro. Endocrinology. 2003; 144:2644–2649. [PubMed: 12746328]
25. Arufe MC, et al. Directed differentiation of mouse embryonic stem cells into thyroid follicular cells. Endocrinology. 2006; 147:3007–3015. [PubMed: 16497809]
26. Jiang N, et al. Differentiation of E14 mouse embryonic stem cells into thyrocytes in vitro. Thyroid. 2010; 20:77–84. [PubMed: 19886789]
27. Longmire TA, et al. Efficient derivation of purified lung and thyroid progenitors from embryonic stem cells. Cell Stem Cell. 2012; 10:398–411. [PubMed: 22482505]
28. Gruters A, Krude H. Detection and treatment of congenital hypothyroidism. Nat Rev Endocrinol. 2012; 8:104–113. [PubMed: 22009163]
29. Bondue A, et al. Mesp1 Acts as a Master Regulator of Multipotent Cardiovascular Progenitor Specification. Cell Stem Cell. 2008; 3:69–84. [PubMed: 18593560]
30. Abel ED, et al. Divergent roles for thyroid hormone receptor beta isoforms in the endocrine axis and auditory system. J Clin Invest. 1999; 104:291–300. [PubMed: 10430610]
31. Rodriguez W, et al. Deletion of the RNaseIII enzyme dicer in thyroid follicular cells causes hypothyroidism with signs of neoplastic alterations. PLoS ONE. 2012; 7:e29929. [PubMed: 22242190]
32. Poulsom R, et al. Bone marrow contributes to renal parenchymal turnover and regeneration. J Pathol. 2001; 195:229–235. [PubMed: 11592103]
33. Pohlenz J, et al. Improved radioimmunoassay for measurement of mouse thyrotropin in serum: strain differences in thyrotropin concentration and thyrotroph sensitivity to thyroid hormone. Thyroid. 1999; 9:1265–1271. [PubMed: 10646670]

NIH-PA Author Manuscript
NIH-PA Author Manuscript
NIH-PA Author Manuscript

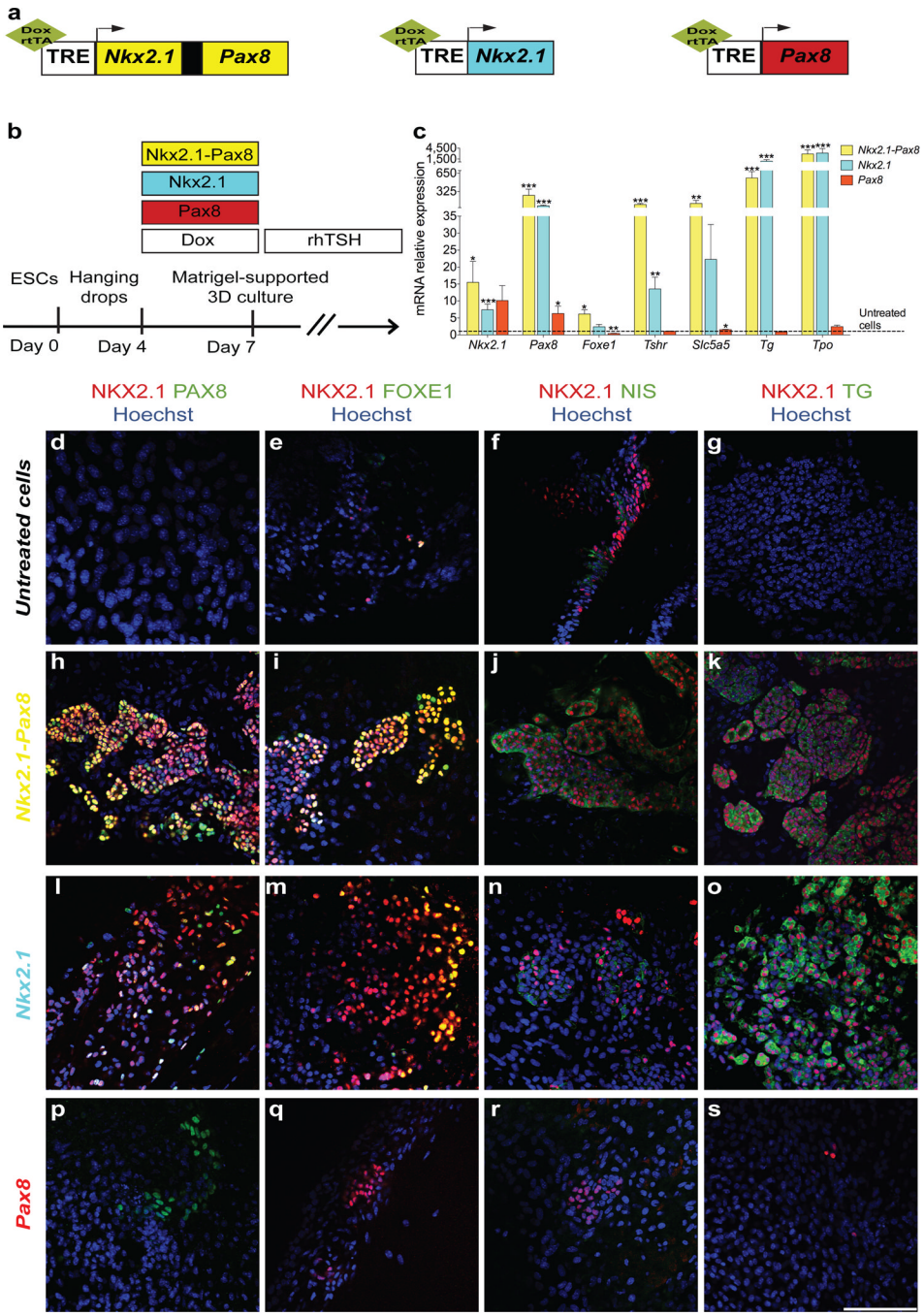

Figure 1. Ectopic expression of *Nkx2.1* and *Pax8* promotes the differentiation of mESCs into thyroid follicles

a, Schematic representation of tetracycline-inducible mESC lines. **b,** Schematic diagram of thyroid follicle differentiation protocol from mESCs. **c,** Expression of endogenous *Nkx2.1* and *Pax8*, *Foxe1, Tshr, Slc5a5, Tg* and *Tpo* at day 22 in cells differentiated after Dox-mediated induction of *Nkx2.1-Pax8* (yellow columns), *Nkx2.1* (cyan columns) and *Pax8* (red columns). Relative expression of each transcript is presented as fold change compared to untreated cells at day 22 as mean ± s.e.m. ($n = 6$). Unpaired *t*-test was used for statistical analysis. $*P < 0.05$, $**P < 0.01$, $***P < 0.001$. **d–s**, Immunostaining at day 22 of untreated cells (**d–g**) and after Dox-mediated induction of *Nkx2.1-Pax8* (**h–k**), *Nkx2.1* (**l–o**) and *Pax8*

(**p–s**) for NKX2.1/PAX8 (**d,h,l,p**), NKX2.1/FOXE1 (**e,i,m,q**), NKX2.1/NIS (**f,j,n,r**) and NKX2.1/TG (**g,k,o,s**). Scale bar, 100 μm (**d–s**).

NIH-PA Author Manuscript
NIH-PA Author Manuscript
NIH-PA Author Manuscript

NIH-PA Author Manuscript
NIH-PA Author Manuscript
NIH-PA Author Manuscript

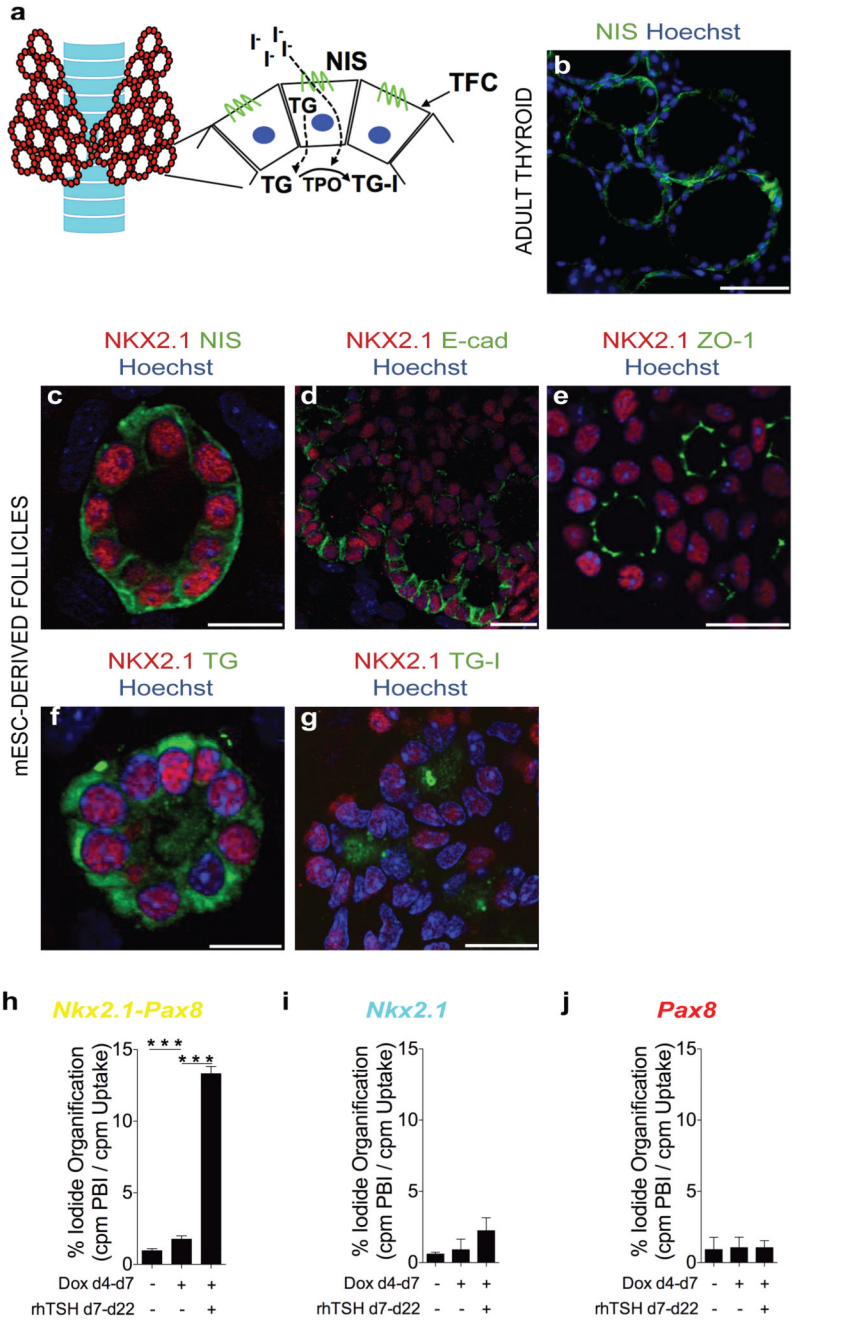

Figure 2. mESC-derived thyroid cells show full morphological and functional maturation

a, Schematic diagram of thyroid gland organised in follicles. **b,** Immunostaining of NIS in adult thyroid tissue. **c–f,** Immunofluorescence at day 22 of thyroid follicles derived from mESCs upon ectopic expression of *Nkx2.1* and *Pax8* for NKX2.1/NIS (**c**), NKX2.1/E-cad (**d**), NKX2.1/ZO-1 (**e**) and NKX2.1/TG (**f**). **g,** Immunodetection of iodinated TG (TG-I) in the luminal compartment of NKX2.1-positive follicles. **h–j,** Iodide organification assay in cells differentiated after Dox-induction of *Nkx2.1-Pax8* (**h**), *Nkx2.1* (**i**) and *Pax8* (**j**). Histograms show the organification percentage of iodine-125 at day 22 in cells differentiated without Dox and rhTSH (left column), in presence of Dox only (central

column) and upon Dox and rhTSH treatment (right column). Data are presented as mean ± s.e.m. ($n = 3$). Tukey's Multiple Comparison Test was used for statistical analysis. ***$P < 0.001$. Scale bars, 200 μm (**b**) and 20 μm (**c–g**).

NIH-PA Author Manuscript
NIH-PA Author Manuscript
NIH-PA Author Manuscript

NIH-PA Author Manuscript

NIH-PA Author Manuscript

NIH-PA Author Manuscript

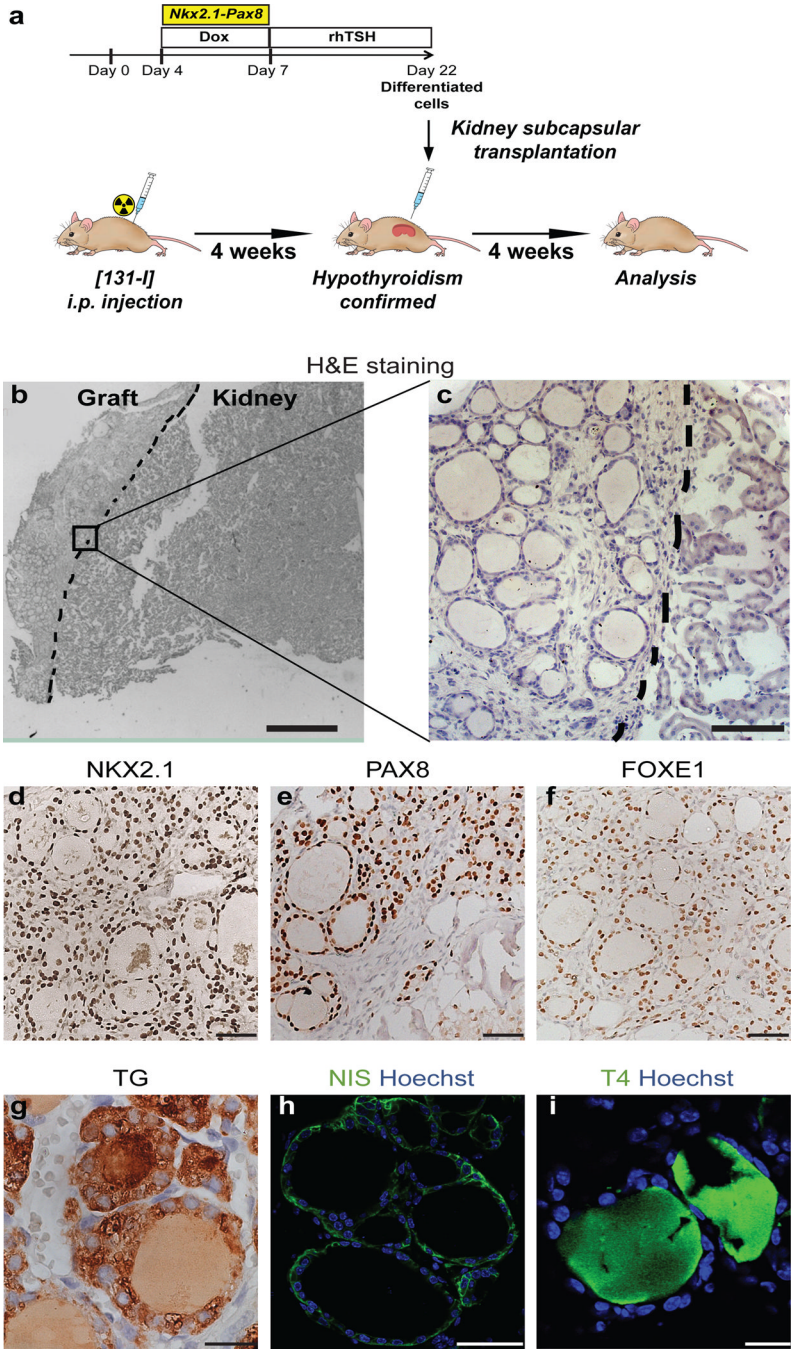

Figure 3. Grafting of mESC-derived thyroid follicles in mice

a, Schematic diagram of protocol for mESC-derived thyroid follicles transplantation in the renal capsule of mice with radio-ablated thyroid (hypothyroid mice). **b–i,** Histological analysis of kidneys sections 4 weeks after grafting. Hematoxylin and eosin staining (H&E) on OCT-embedded grafted kidney showed: - localization of transplanted tissue in the cortical area of the host organ (left side) (**b**) - and single cuboidal epithelium organization of transplanted tissue (**c**); Immunohistochemistry of NKX2.1 (**d**), PAX8 (**e**), FOXE1 (**f**), TG (**g**), and immunofluorescence of NIS (**h**) and T4 (**i**) in grafted tissue. Scale bars 300 μm (**b**), 100 μm (**c**), 50 μm (**d,e,f,h**) and 20 μm (**g,i**).

NIH-PA Author Manuscript

NIH-PA Author Manuscript

NIH-PA Author Manuscript

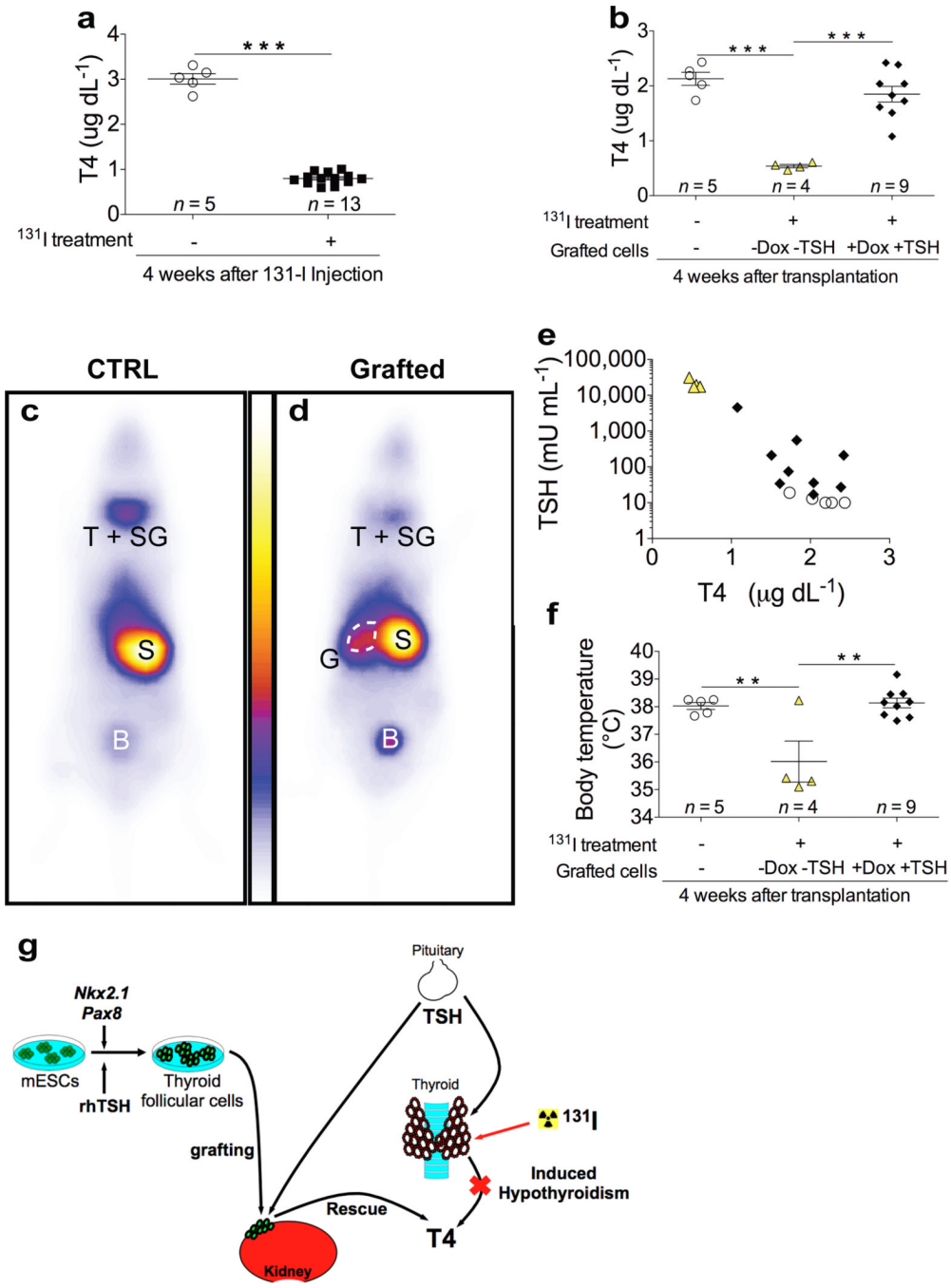

Figure 4. Rescue of experimentally induced hypothyroidism by transplanting mESC-derived thyroid follicles

a, Plasma total T4 level 4 weeks after injection in untreated (open circles) and iodine-131 treated (black squares) mice. **b**, Plasma total T4 level 4 weeks after transplantation of differentiated cells in iodine-131 treated mice. **c–d,** Whole-body images of mice 30 minutes after the injection of ^{99m}Tc-pertechnate. 4 weeks after grafting, body scan was performed on untreated control mice (CTRL) (**c**) or iodine-131 treated mice grafted with mESC-derived follicles (Grafted) (**d**); T+SG, thyroid and salivary glands; S, stomach; B, bladder; G, grafted mESC-derived follicles (G). **e**, Relationship between plasma TSH and T4 levels 4 weeks after grafting. **f**, Body temperature measurements 4 weeks after grafting. In **b**,**e**,**f,** open

NIH-PA Author Manuscript

NIH-PA Author Manuscript

NIH-PA Author Manuscript

circles show iodine-131 untreated and ungrafted mice; yellow triangles show mice treated with iodine-131 and grafted with cells differentiated without Dox and rhTSH (-Dox-TSH); black diamonds show mice treated with iodine-131 and grafted with cells differentiated with Dox and rhTSH (+Dox+TSH). The values are shown as *dot plot* (**a**,**b**,**f**) or *scatter plot* (**e**) and as mean ± s.e.m.. Unpaired *t*-test (**a**) and Tukey's Multiple Comparison Test (**b,f**) were used for statistical analysis. $^{**}P < 0.01$, $^{***}P < 0.001$**. g**, Graphical summary: *Nkx2.1* and *Pax8* co-expression in combination with rhTSH treatment leads to differentiation of mESC into fully functional thyroid follicles that promote *in vivo* hormonal and symptomatic recovery of hypothyroid state.